

THE LSND PUZZLE IN THE LIGHT OF MINIBOONE RESULTS

THOMAS SCHWETZ

Physics Department, Theory Division, CERN, CH-1211 Geneva 23, Switzerland

I give a brief overview over various attempts to reconcile the LSND evidence for oscillations with all other global neutrino data, including the results from MiniBooNE. I discuss the status of oscillation schemes with one or more sterile neutrinos and comment on various exotic proposals.

1 Introduction

Reconciling the LSND evidence¹ for $\bar{\nu}_\mu \rightarrow \bar{\nu}_e$ oscillations with the global neutrino data reporting evidence and bounds on oscillations remains a long-standing problem for neutrino phenomenology. Recently the MiniBooNE experiment^{2,3} added more information to this question. This experiment searches for $\nu_\mu \rightarrow \nu_e$ appearance with a very similar L/E_ν range as LSND. No evidence for flavour transitions is found in the energy range where a signal from LSND oscillations is expected ($E > 475$ MeV), whereas an event excess is observed below 475 MeV at a significance of 3σ . Two-flavour oscillations cannot account for such an excess and currently the origin of this excess is under investigation², see also⁴. MiniBooNE results are inconsistent with a two-neutrino oscillation interpretation of LSND at 98% CL³, see also⁵. The exclusion contour from MiniBooNE is shown in Fig. 1 (left) in comparison to the LSND allowed region and the previous bound from the KARMEN experiment⁶, all in the framework of 2-flavour oscillations.

2 Sterile neutrino oscillations

The standard “solution” to the LSND problem is to introduce one or more sterile neutrinos at the eV scale in order to provide the required mass-squared difference to accommodate the LSND signal in addition to “solar” and “atmospheric” oscillations. However, in such schemes there is severe tension between the LSND signal and short-baseline disappearance experiments, most importantly Bugey⁷ and CDHS⁸, with some contribution also from atmospheric neutrino data⁹.

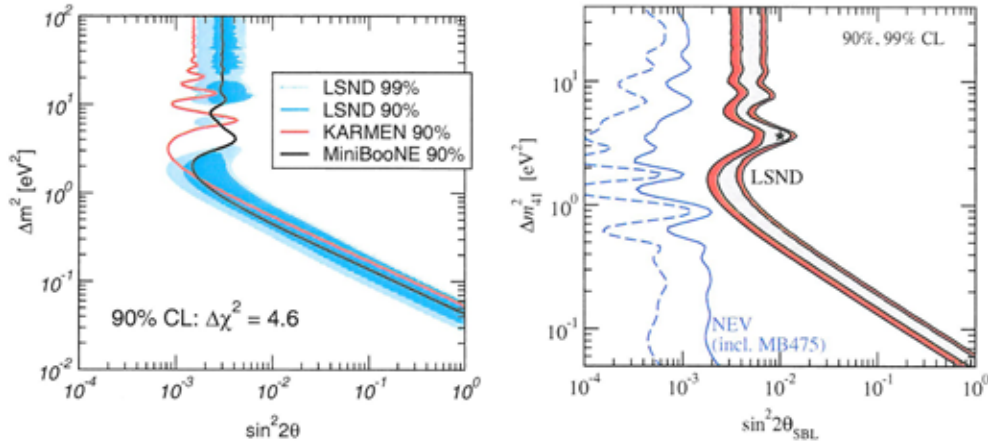


Figure 1: Left: Two-neutrino exclusion contours at 90% C.L. (2 d.o.f.) for MiniBooNE and KARMEN compared to the LSND allowed region at 90% and 99% C.L. For all three experiments the same $\Delta\chi^2$ cut has been used to define the 90% C.L. region. Right: Constraint on the LSND mixing angle in (3+1) schemes from no-evidence appearance and disappearance experiments (NEV) at 90% and 99% C.L. The shaded region corresponds to the allowed region from LSND decay-at-rest data.

I report here the results from a global analysis including MiniBooNE data within schemes with one, two and three sterile neutrinos¹⁰.

Four-neutrino oscillations within so-called (3+1) schemes have been only marginally allowed before the recent MiniBooNE results^{11,12,13}, and become even more disfavored with the new data. We find that the LSND signal is disfavoured by all other null-result short-baseline appearance and disappearance experiments (including MiniBooNE) at the level of 4σ ¹⁰. The corresponding upper bound on the effective LSND mixing angle is shown in Fig. 1 (right). Five-neutrino oscillations in (3+2) schemes¹³ allow for the possibility of CP violation in short-baseline oscillations¹⁴. Using the fact that in LSND the signal is in anti-neutrinos, whereas present MiniBooNE data is based on neutrinos, these two experiments become fully compatible in (3+2) schemes¹⁰. Moreover, in principle there is enough freedom to obtain the low energy excess in MiniBooNE and being consistent at the same time with the null-result in the high energy part as well as with the LSND signal, see Fig. 2 (left, red histogram). However, in the global analysis the tension between appearance and disappearance experiments remains unexplained. This problem is illustrated in Fig. 2 (right) where sections through the allowed regions in the parameter space for appearance and disappearance experiments are shown. An opposite trend is clearly visible: while appearance data require non-zero values for the mixing of ν_e and ν_μ with the eV-scale mass states 4 and 5 in order to explain LSND, disappearance data provide an upper bound on this mixing. The allowed regions touch each other at $\Delta\chi^2 = 9.3$, and a consistency test between these two data samples yields a probability of only 0.18%, i.e., these models can be considered as disfavored at the 3σ level¹⁰. Also, because of the constraint from disappearance experiments the low energy excess in MiniBooNE can not be explained in the global analysis, see Fig. 2 (left, blue histogram). Furthermore, when moving from 4 neutrinos to 5 neutrinos the fit improves only by 6.1 units in χ^2 by introducing 4 more parameters, showing that in (3+2) schemes the tension in the fit remains a severe problem. This is even true in the case of three sterile neutrinos, since adding one more neutrino to (3+2) cannot improve the situation¹⁰.

3 Exotic proposals

Triggered by these problems many ideas have been presented in order to explain LSND, some of them involving very speculative physics, among them sterile neutrino decay^{15,16}, violation

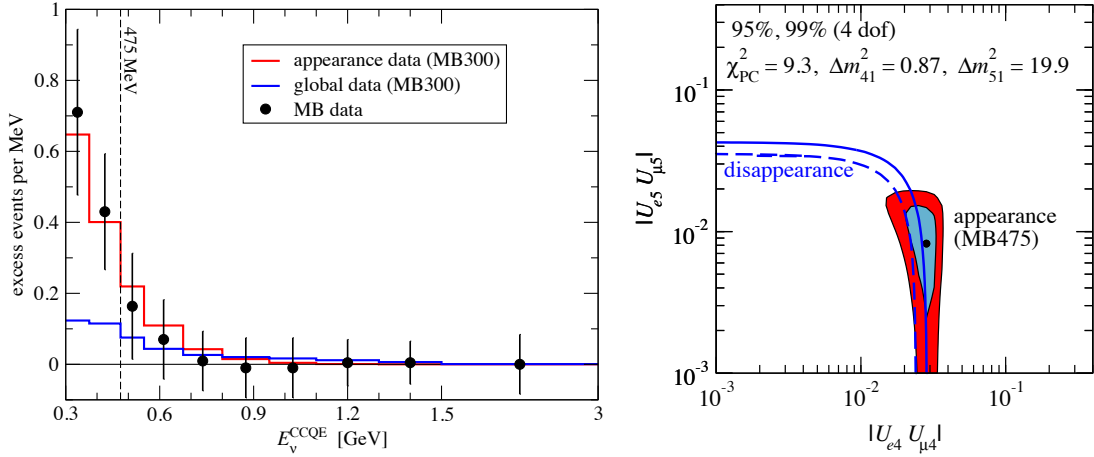


Figure 2: Left: Best fit spectra in (3+2) oscillations for MiniBooNE using appearance data only (MB, LSND, KARMEN, NOMAD) as well as in the global fit. Right: Section of the 4-dimensional volumes allowed at 95% and 99% CL in the (3+2) scheme from SBL appearance and disappearance experiments in the space of the parameters in common to these two data sets. The values of Δm_{41}^2 and Δm_{51}^2 of the displayed sections correspond to the point in parameter space where the two allowed regions touch each other (at a $\Delta\chi^2 = 9.3$).

of the CPT^{17,12,18,19} and/or Lorentz²⁰ symmetries, quantum decoherence^{21,22,23} mass-varying neutrinos²⁴, short-cuts of sterile neutrinos in extra dimensions²⁵, a non-standard energy dependence of sterile neutrinos²⁶, or sterile neutrinos interacting with a new gauge boson²⁷. In the following I comment on a personal selection of these exotic proposals, without the ambition of being complete.

CPT violation. Triggered by the observation that the LSND signal is in anti-neutrinos, whereas their neutrino data is consistent with no oscillations, it was proposed¹⁷ that neutrinos and anti-neutrinos have different masses and mixing angles, which violates the CPT symmetry. A first challenge to this idea has been the KamLAND reactor results, which require a Δm^2 at the solar scale for anti-neutrinos. Subsequently it has been shown that the oscillation signature in SuperK atmospheric neutrino data (which cannot distinguish between ν and $\bar{\nu}$ events) is strong enough to require a $\Delta m^2 \sim 2.5 \cdot 10^{-3} \text{ eV}^2$ for neutrinos as well as for anti-neutrinos¹⁸, see²⁸ for an update. This rules out such an explanation of the LSND signal with three neutrinos at 4.6σ . However, introducing a sterile neutrino, and allowing for different masses and mixings for neutrinos and anti-neutrinos¹⁹ is fully consistent with all data, including the MiniBooNE null-result in neutrinos. Such a model should lead to a positive signal in the MiniBooNE anti-neutrino run.

Sterile neutrino decay. Pre-MiniBooNE data can be fitted under the hypothesis¹⁶ of a sterile neutrino, which is produced in pion and muon decays because of a small mixing with muon neutrinos, $|U_{\mu 4}| \simeq 0.04$, and then decays into an invisible scalar particle and a light neutrino, predominantly of the electron type. One needs values of $gm_4 \sim \text{few eV}$, g being the neutrino–scalar coupling and m_4 the heavy neutrino mass, e.g. m_4 in the range from 1 keV to 1 MeV and $g \sim 10^{-6}–10^{-3}$. This minimal model is in conflict with the null-result of MiniBooNE. It is possible to save this idea by introducing a second sterile neutrino, such that the two heavy neutrinos are very degenerate in mass. If the mass difference is comparable to the decay width, CP violation can be introduced in the decay, and the null-result of MiniBooNE can be reconciled with the LSND signal¹⁶.

Sterile neutrinos with an exotic energy dependence. Short-baseline data can be divided into low-energy (few MeV) reactor experiments, LSND and KARMEN around 40 MeV, and the high-energy (GeV range) experiments CDHS, MiniBooNE, NOMAD. Based on this observation it turns out that the problems of the fit in (3+1) schemes can be significantly alleviated if one

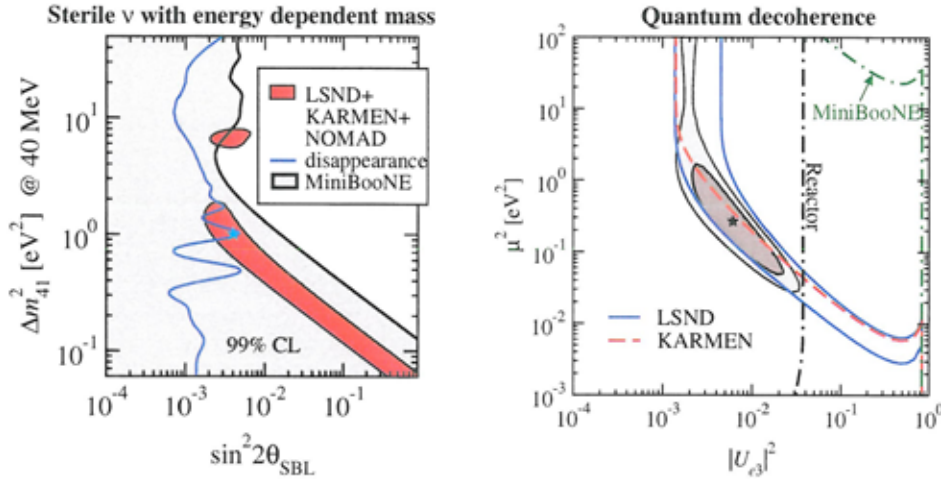


Figure 3: Left: Bounds from disappearance experiments and MiniBooNE compared to the LSND region for (3+1) oscillations when the sterile neutrino mass depends on energy as $m_4^2(E_\nu) \propto E_\nu^{-0.3}$. Right: Quantum decoherence in three-active neutrino oscillations. Lines correspond to 99% CL regions of individual experiments, shaded regions show the 90% and 99% CL region of the global analysis, and the star marks the best fit point. The parameter μ is defined by parameterizing the decoherence parameter γ as $\gamma = \mu^2/E_\nu$ (40 MeV/ E_ν) 3 .

assumes that the mass or the mixing of the sterile neutrino depend on its energy in an exotic way²⁶. For example, assuming that $m_4^2(E_\nu) \propto E_\nu^{-r}$ one finds that for $r > 0$ the MiniBooNE exclusion curve is shifted to larger values of Δm^2 , whereas the bound from disappearance experiments is moved towards larger values of the mixing angle, and hence the various data sets become consistent with LSND, compare Fig. 3 (left). At the best fit point with $r \simeq 0.3$ the global fit improves by 12.7 units in χ^2 with respect to the standard (3+1) fit. Similar improvement can be obtained if energy dependent mixing of the sterile neutrino is assumed.²⁶

Let us note that this is a purely phenomenological observation, and it seems difficult to construct explicit models for such sterile neutrinos. There are models which effectively introduce a non-standard “matter effect” for sterile neutrinos, *e.g.* via exotic extra dimensions²⁵ or via postulating a new gauge interaction of the sterile neutrinos²⁷. Similar as in the usual MSW case, the sterile neutrino encounters effective mass and mixing which depend on energy. However, in these approaches the matter effect felt by the sterile state has to be some orders of magnitude larger than the standard weak-force matter effect of active neutrinos, in order to be relevant for short-baseline experiments. In such a case, in general very large effects are expected for long-baseline experiments such as MINOS, atmospheric neutrinos, or KamLAND. Unfortunately an explicit demonstration that a successful description of all these data can be maintained in such models is still lacking.

Quantum decoherence. The possibility that the origin of the LSND signal might be quantum decoherence in neutrino oscillations has been considered in^{21,22,23}. Such effects can be induced by interactions with a stochastic environment; a possible source for this kind of effect might be quantum gravity. The attempts to explain the LSND signal by quantum decoherence in^{21,22} seem to be in conflict with present data. Both of these models are ruled out by the bound from NuTeV, $P_{\nu_\mu \rightarrow \nu_e}, P_{\bar{\nu}_\mu \rightarrow \bar{\nu}_e} < 5 \times 10^{-4}$ (90% C.L.)²⁹. Furthermore, the model of²¹ (where in addition to decoherence, CPT-violation is also introduced which results in a difference between the oscillation probabilities for neutrinos and anti-neutrinos) cannot account for the spectral distortion in the anti-neutrino signal observed by KamLAND, whereas the scenario of²² is disfavored by the absence of a signal in KARMEN, NOMAD and MiniBooNE.

Recently we have revisited this idea²³ by introducing a different set of decoherence parameters. We assume that only the neutrino mass state ν_3 is affected by decoherence, whereas the 1-2

sector is completely unaffected, guaranteeing the standard explanation of solar and KamLAND data. Hence, denoting as γ_{ij} the parameter which controls the decohering of the mass states ν_i and ν_j , we have $\gamma_{12} = 0$ and $\gamma_{13} = \gamma_{23} \equiv \gamma$, where we have assumed that decoherence effects are diagonal in the mass basis. Furthermore, we assume that decoherence effects are suppressed for increasing neutrino energies, $\propto E_\nu^{-r}$ with $r \sim 4$. This makes sure that at short-baseline experiments with $E_\nu \gtrsim 1$ GeV such as MiniBooNE, CDHS, NOMAD, and NuTeV no signal is predicted, and at the same time maintains standard oscillations for atmospheric data and MINOS. In this way a satisfactory fit to the global data is obtained. Disappearance and appearance data become fully compatible with a probability of 74%, compared to 0.2% in the case of (3+2) oscillations. The LSND signal is linked to the mixing angle θ_{13} , see Fig. 3(right) and hence, this scenario can be tested at upcoming θ_{13} searches: while the comparison of near and far detector measurements at reactors should lead to a null-result because of strong damping at low energies, a positive signal for θ_{13} is expected in long-baseline accelerator experiments.

4 Outlook

Currently MiniBooNE is taking data with anti-neutrinos.² This measurement is of crucial importance to test scenarios involving CP (such as (3+2) oscillations) or even CPT violation to reconcile LSND and present MiniBooNE data. Therefore, despite the reduced flux and detection cross section of anti-neutrinos the hope is that enough data will be accumulated in order to achieve good sensitivity in the anti-neutrino mode. Furthermore, it is of high importance to settle the origin of the low energy excess in MiniBooNE. If this effect persists and does not find an “experimental” explanation such as an over-looked background, an explanation in terms of “new physics” seems to be extremely difficult. To the best of my knowledge, so-far no convincing model able to account for the sharp rise with energy while being consistent with global data has been provided yet.

The main goal of upcoming oscillation experiments like Double-Chooz, Daya Bay, T2K, NO ν A is the search for the mixing angle θ_{13} , with typical sensitivities of³⁰ $\sin^2 2\theta_{13} \gtrsim 1\%$. This should be compared to the size of the appearance probability observed in LSND: $P_{\text{LSND}} \approx 0.26\%$. Hence, if θ_{13} is large enough to be found in those experiments sterile neutrinos may introduce some sub-leading effect, but their presence cannot be confused with a non-zero θ_{13} . Nevertheless, I argue that it could be worth to look for sterile neutrino effects in the next generation of experiments. They would introduce (mostly energy averaged) effects, which could be visible as disappearance signals in the near detectors of these experiments. This has been discussed³¹ for the Double-Chooz experiment, but also the near detectors at superbeam experiments should be explored. An interesting effect of (3+2) schemes has been pointed out recently for high energy atmospheric neutrinos in neutrino telescopes³². The crucial observation is that for $\Delta m^2 \sim 1 \text{ eV}^2$ the MSW resonance occurs around TeV energies, which leads to large effects for atmospheric neutrinos in this energy range, potentially observable at neutrino telescopes. Another method to test sterile neutrino oscillations would be to put a radioactive source inside a detector with good spatial resolution, which would allow to observe the oscillation pattern within the detector³³. I stress that in a given exotic scenario such as the examples discussed in sec. 3 signatures in up-coming experiments might be different than for “conventional” sterile neutrino oscillations.

For the subsequent generation of oscillation experiments aiming at sub-percent level precision to test CP violation and the neutrino mass hierarchy, the question of LSND sterile neutrinos is highly relevant^{34,35}. They will lead to a miss-interpretation or (in the best case) to an inconsistency in the results. If eV scale steriles exist with mixing relevant for LSND the optimization in terms of baseline and E_ν of high precision experiments has to be significantly changed. Therefore, I argue that it is important to settle this question at high significance before decisions on high precision oscillation facilities are taken.

References

1. A. Aguilar *et al.* [LSND Coll.], Phys. Rev. D **64**, 112007 (2001) [hep-ex/0104049].
2. C. Polly, these proceedings.
3. A. A. Aguilar-Arevalo *et al.* [MiniBooNE Coll.], Phys. Rev. Lett. **98**, 231801 (2007).
4. R. Hill, these proceedings; J. A. Harvey, C. T. Hill and R. J. Hill, Phys. Rev. Lett. **99** (2007) 261601 [0708.1281].
5. A. A. Aguilar-Arevalo *et al.* [MiniBooNE Coll.], 0805.1764 [hep-ex].
6. B. Armbruster *et al.* [KARMEN Coll.], Phys. Rev. D **65**, 112001 (2002) [hep-ex/0203021].
7. Y. Declais *et al.*, Nucl. Phys. B **434**, 503 (1995).
8. F. Dydak *et al.*, Phys. Lett. B **134**, 281 (1984).
9. S. M. Bilenky, C. Giunti, W. Grimus and T. Schwetz, Phys. Rev. D **60**, 073007 (1999) [hep-ph/9903454].
10. M. Maltoni and T. Schwetz, Phys. Rev. D **76** (2007) 093005 [0705.0107].
11. M. Maltoni, T. Schwetz, M. A. Tortola and J. W. F. Valle, Nucl. Phys. B **643**, 321 (2002) [hep-ph/0207157].
12. A. Strumia, Phys. Lett. B **539**, 91 (2002) [hep-ph/0201134].
13. M. Sorel, J. M. Conrad and M. Shaevitz, Phys. Rev. D **70**, 073004 (2004) [hep-ph/0305255].
14. G. Karagiorgi *et al.*, Phys. Rev. D **75**, 013011 (2007) [hep-ph/0609177]; J. T. Goldman, G. J. Stephenson and B. H. J. McKellar, Phys. Rev. D **75** (2007) 091301.
15. E. Ma, G. Rajasekaran and I. Stancu, Phys. Rev. D **61**, 071302 (2000) [hep-ph/9908489]; E. Ma and G. Rajasekaran, Phys. Rev. D **64**, 117303 (2001) [hep-ph/0107203].
16. S. Palomares-Ruiz, S. Pascoli and T. Schwetz, JHEP **0509**, 048 (2005) [hep-ph/0505216].
17. H. Murayama and T. Yanagida, Phys. Lett. B **520**, 263 (2001) [hep-ph/0010178]; G. Barenboim, L. Borissoff and J. Lykken, hep-ph/0212116.
18. M. C. Gonzalez-Garcia, M. Maltoni and T. Schwetz, Phys. Rev. D **68**, 053007 (2003) [hep-ph/0306226].
19. V. Barger, D. Marfatia and K. Whisnant, Phys. Lett. B **576**, 303 (2003) [hep-ph/0308299].
20. V. A. Kostelecky and M. Mewes, Phys. Rev. D **70**, 076002 (2004) [hep-ph/0406255]; A. de Gouvea and Y. Grossman, Phys. Rev. D **74**, 093008 (2006) [hep-ph/0602237]; T. Katori, A. Kostelecky and R. Tayloe, Phys. Rev. D **74**, 105009 (2006) [hep-ph/0606154].
21. G. Barenboim and N. E. Mavromatos, JHEP **0501** (2005) 034 [hep-ph/0404014].
22. G. Barenboim, N. E. Mavromatos, S. Sarkar and A. Waldron-Lauda, Nucl. Phys. B **758** (2006) 90 [hep-ph/0603028].
23. Y. Farzan, T. Schwetz and A. Yu. Smirnov, 0805.2098 [hep-ph].
24. D. B. Kaplan, A. E. Nelson and N. Weiner, Phys. Rev. Lett. **93**, 091801 (2004) [hep-ph/0401099]; K. M. Zurek, JHEP **0410**, 058 (2004) [hep-ph/0405141]; V. Barger, D. Marfatia and K. Whisnant, Phys. Rev. D **73**, 013005 (2006) [hep-ph/0509163].
25. H. Pas, S. Pakvasa and T. J. Weiler, Phys. Rev. D **72**, 095017 (2005) [hep-ph/0504096].
26. T. Schwetz, JHEP **0802** (2008) 011 [0710.2985].
27. A. Nelson, these proceedings; A. E. Nelson and J. Walsh, 0711.1363 [hep-ph].
28. M. C. Gonzalez-Garcia and M. Maltoni, Phys. Rept. **460** (2008) 1 [0704.1800].
29. S. Avvakumov *et al.*, Phys. Rev. Lett. **89** (2002) 011804 [hep-ex/0203018].
30. P. Huber, M. Lindner, M. Rolinec, T. Schwetz and W. Winter, Phys. Rev. D **70** (2004) 073014 [hep-ph/0403068].
31. A. Bandyopadhyay and S. Choubey, 0707.2481 [hep-ph].
32. S. Choubey, JHEP **0712** (2007) 014 [0709.1937].
33. C. Grieb, J. Link and R. S. Raghavan, Phys. Rev. D **75**, 093006 (2007) [hep-ph/0611178].
34. A. Donini, M. Lusignoli and D. Meloni, Nucl. Phys. B **624** (2002) 405 [hep-ph/0107231].
35. A. Dighe and S. Ray, Phys. Rev. D **76** (2007) 113001 [0709.0383].